

Experimental and theoretical study of magnetodons in GaAs and InP at megagauss fields

W. Zawadzki*

Institut für Halbleiterphysik, Kepler Universität, A-4040 Linz, Austria

P. Pfeffer

Institute of Physics, Polish Academy of Sciences, 02668-Warsaw, Poland

S. P. Najda,[†] H. Yokoi, S. Takeyama, and N. Miura

Institute for Solid State Physics, University of Tokyo, Roppongi 7-22-1, Tokyo 106, Japan

(Received 29 June 1993)

Donor states in GaAs and InP at megagauss magnetic fields are studied experimentally and theoretically. The data allow us to investigate the magnetodons for values of $\gamma = \hbar\omega_c / 2 \text{ Ry}^* \approx 10$, unattainable until now in these materials. The observations are described by a theoretical model, which uses variational atomic-magnetic wave functions and accounts for the band nonparabolicity within an effective two-band $\mathbf{k} \cdot \mathbf{p}$ formalism. The theory describes well the absolute values and field dependences of energy shifts between the cyclotron resonance (CR) transitions and the corresponding magnetodonor impurity cyclotron resonance (ICR) transitions in both materials. Spin doublets of CR and ICR transitions are considered; they are shown to be related to a variation of the spin g value with the energy. It is argued that the spin-doublet splittings at high fields should be considerably larger in GaAs than in InP. This conclusion agrees with the observations.

I. INTRODUCTION

Magnetodonor (MD) states in semiconductors have been the subject of sustained experimental and theoretical interest due to their physical properties as well as important applications, most notably in infrared detection.¹ Magnetodonor investigations have been used to determine the static dielectric constant of material, to identify the chemical nature of impurities, to study screening properties of the electron gas, to investigate the metal-nonmetal transition, etc. Magneto-optical and magneto-transport investigations proved to be useful in determining the positions of donors in modulation-doped two-dimensional structures, which is important for device applications.

The importance of the MD system goes beyond semiconductor physics, however, since a magnetodonor imitates the hydrogen atom in a large magnetic field.² The problem of an electron subjected to simultaneous Coulomb and magnetic-field interaction is characterized by the parameter

$$\gamma = \frac{\hbar\omega_c}{2 \text{ Ry}^*} = \left(\frac{a_B^*}{L} \right)^2, \quad (1)$$

where $\omega_c = eB/m_0^*$ is the cyclotron frequency, $L = (\hbar/eB)^{1/2}$ is the magnetic radius, and a_B^* is the effective Bohr radius. At achievable magnetic fields the value of γ is of the order of 10^{-5} for the hydrogen atom in vacuum. In narrow-gap semiconductors, which have small effective masses and high dielectric constants, γ can reach values of 100 or more. The formal identity between the magnetodonor and the hydrogen atom in the presence of a very strong magnetic field makes the problem of

interest to astrophysicists and atomic physicists (cf. Ref. 3 and the references therein).

Theoretically, the magnetodonor problem has turned out to be a real challenge since, even in the simplest case of a parabolic and spherical energy band, the eigenvalue equation does not seem to have closed solutions. Thus, numerous methods have been devised to obtain suitable approximations for the eigenenergies and eigenfunctions at low, intermediate, and high γ values (cf. review by Zawadzki, Ref. 4).

In the present paper we are interested in the MD states in GaAs and InP at megagauss fields, which in these materials correspond to $\gamma \approx 10$. To our knowledge, the existing literature data do not consider cases where γ exceeds about 2. Kaplan⁵ demonstrated the universality of the MD formulation in terms of γ comparing the results for GaAs and InSb. Poehler⁶ investigated the ground-state MD binding energy in GaAs using the magnetic freeze-out effect. Kadri *et al.*⁷ performed a similar experiment with InP in fields up to 18 T. Sigg, Bluysen, and Wyder⁸ and Zawadzki, Pfeffer, and Sigg⁹ studied the MD states in GaAs related to the donor-shifted cyclotron resonance in fields up to 22.5 T and showed that a marked nonparabolicity of the conduction band is to be accounted for in the description of the data. Armistead, Stradling, and Wasilewski¹⁰ observed magneto-optical transitions to high excited MD states in GaAs. Theoretically, the effect of the band's nonparabolicity on the ground MD state has been studied by Larsen¹¹ and generalized to other states by Zawadzki and Wlasak¹² (cf. also Zawadzki *et al.* Ref. 13). Modifications of the MD behavior for donors placed inside quantum wells,¹⁴⁻¹⁶ as well as outside the wells^{17,18} in GaAs-Ga_{1-x}Al_xAs system have been studied experimentally and theoretically.

Our paper is organized in the following way. In Sec. II we consider atomic-magnetic variational functions for the MD states and describe a theoretical model applying to the conduction bands of GaAs and InP, Sec. III presents the experimental MD data for both materials at megagauss fields, and in Sec. IV we compare the theory with experiment and discuss the conclusions.

II. THEORY

We divide the theoretical description into two parts. First, we consider atomic-magnetic variational functions for magnetodonors at medium γ values and check their quality in the standard case of parabolic and spherical energy band, which permits a direct comparison with existing theories. Second, we discuss the MD states associated with real conduction bands of GaAs and InP.

A. Atomic-magnetic trial functions

We consider atomic-magnetic trial functions, first proposed by Pokatilov and Rusanov¹⁹ (cf. also Ref. 20). These functions combine atomic and magnetic features, allowing one to calculate the MD energies with sufficient accuracy without referring to heavy numerics. The functions are labeled by three quantum numbers $NM\beta$, where $N=0,1,2,\dots$, $M=\dots,-1,0,1,\dots$ is the projection of the angular momentum on the field direction, and $\beta=0,1,2,\dots$ quantizes the motion in the z direction. The quantum number of the Landau subband to which the given MD state “belongs” at high fields is $n=N+(M+|M|)/2$. Other notations are also in use cf. Ref. 4.

The ground MD state and two important excited states are described by the wave functions (in cylindrical coordinates)

$$\Psi_{000} = C \exp(-a\rho^2 - br), \quad (2)$$

$$\Psi_{0\bar{1}0} = C \exp(-i\varphi)\rho \exp(-a\rho^2 - br), \quad (3)$$

$$\Psi_{010} = C \exp(+i\varphi)\rho \exp(-a\rho^2 - br), \quad (4)$$

where $r=(\rho^2+z^2)^{1/2}$. The normalization coefficients C and the variational parameters a and b take different values for different functions. The “atomic” factor is $\exp(-br)$, while $\exp(-a\rho^2)$ represents the “magnetic” factor (the latter appears in all MD trial functions, cf. Ref. 4). One expects that for $\gamma \ll 1$ the trial functions should be atomiclike (which corresponds to small values of the a parameter), while for $\gamma \gg 1$ the trial functions should be magneticlike (small values of the b parameter).

We first investigate the quality of the above trial functions calculating variational energies for the standard MD Hamiltonian. In effective atomic units (lengths in the Bohr radii $a_B^* = \kappa \hbar^2 / m^* e^2$, energies in the effective Rydbergs $\text{Ry}^* = m^* e^4 / 2\kappa^2 \hbar^2$) the eigenvalue problem reads^{2,4} (spin is omitted)

$$\left[-\nabla^2 - i\gamma \frac{\partial}{\partial \varphi} + \frac{1}{4} \gamma^2 \rho^2 - \frac{2}{\sqrt{\rho^2 + z^2}} \right] \Psi = E \Psi. \quad (5)$$

It is customary to express the calculated MD energy E_{var} as a binding energy, i.e., in relation to the nearest Landau energy $2\gamma(n + \frac{1}{2})$. Thus, for the (000) and (0 $\bar{1}$ 0) states, $E_b = \gamma - E_{\text{var}}$, while for the (010) state, $E_b = 3\gamma - E_{\text{var}}$. For the wave functions (3) and (4) the second term in (5) contributes the value of $-\gamma$ to the energy of the (0 $\bar{1}$ 0) state, and the value of $+\gamma$ to the energy of the (010) state. Thus, the energies of these two states differ by 2γ , so that their corresponding binding energies are exactly the same. In Table I we quote numerical values of the variational binding energies, calculated with the use of the trial functions (2) and (3). These are compared with the values obtained by expansion numerical methods, considered to be “exact.”²¹ It can be seen that for $\gamma \leq 10$, the variational binding energies reproduce the exact values within 2%. However, the observable impurity cyclotron resonance (ICR) energies $E(010) - E(000)$ are described with the precision of about 0.03%, which is largely sufficient for our purposes. The atomic-magnetic wave functions give very good results for $\gamma < 1$, while the magnetic-type functions give rather poor energies in this limit (cf. Refs. 2 and 4).

It is also of interest to calculate the dimensions of the MD states as described by the atomic-magnetic functions. Figure 1 shows longitudinal and transverse radii of the ground MD states versus magnetic field. These have been calculated using the relations

$$\bar{r}_\perp^2 = \int \Psi^* \frac{1}{2} \rho^2 \Psi d^3r, \quad (6)$$

$$\bar{r}_\parallel^2 = \int \Psi^* z^2 \Psi d^3r, \quad (7)$$

for the values of the variational parameters minimizing the energy. It can be seen that, while at $\gamma > 10$ the transverse radius approaches the magnetic radius L , its value

TABLE I. Binding energies (in effective Rydbergs) of two magnetodonor states, as calculated with the use of atomic-magnetic variational functions (left entries). These are compared with the values of Rösner *et al.* [RWHR, Ref. (21)], considered to be exact. For a parabolic band, the binding energy of (010) state is exactly equal to that of (0 $\bar{1}$ 0) state, see text.

γ	(000)		(010)	
	E_b (at-mg)	E_b (RWHR)	E_b (at-mg)	E_b (RWHR)
0.001	1.000 999	1.000 999	0.251 99	0.251 99
0.01	1.009 95	1.009 95	0.269 4	0.269 4
0.1	1.095 05	1.095 05	0.399 14	0.401 7
0.2	1.180 71	1.180 76	0.499 7	0.501 1
0.5	1.393 6	1.393 6	0.695 0	0.695 0
0.6	1.453 7	1.454 9	0.744 5	0.749 2
1	1.659 1	1.662 3	0.905 3	0.913 2
2	2.035 2	2.044 4	1.184 7	1.199 2
3	2.314 0	2.329 1	1.387 2	1.407 1
4	2.541 1	2.561 6	1.551 0	1.575 6
5	2.735 2	2.735 2	1.690 8	1.690 8
10	3.448 4	3.495 6	2.204 7	2.250 8
20	4.351 3	4.430 8	2.860 0	2.930 9
50	5.891 8	5.891 8	3.992 3	3.992 3
100	7.365 7	7.578 1	5.093 6	5.269 5
200	9.151 4	9.453 1	6.446 4	6.694 3

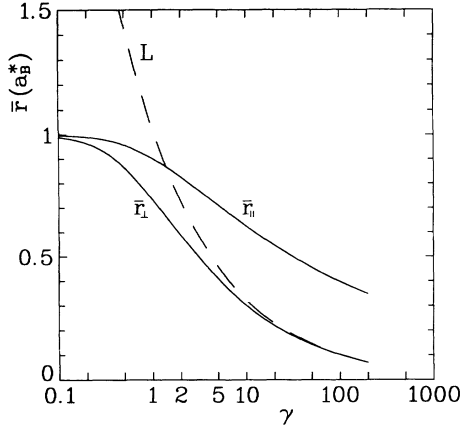


FIG. 1. Transverse and longitudinal radii of the magneto-donor ground state, as described by the atomic-magnetic variational wave function (in units of effective Bohr radius), vs γ .

for $\gamma \rightarrow 0$ tends correctly to the atomic radius a_B^* . This is in contrast to the magnetic-type functions, for which the behavior of \bar{r}_\perp in the limit of $\gamma \rightarrow 0$ is not quite correct.²

B. Description of MD states in GaAs and InP

The reason for using the variational energies rather than the exact ones, as given in Table I, is the nonparabolicity of the conduction bands of GaAs and InP. It has been shown that even at moderate magnetic fields the medium-gap materials GaAs and InP show pronounced nonparabolicity effects.^{22,23} These effects are correspondingly stronger in the megagauss field range and must be accounted for.

The conduction electrons in GaAs and InP at moderate magnetic fields (up to 20 T) have been successfully described with the use of five-level (5L) $\mathbf{k}\cdot\mathbf{p}$ model. However, in the description of MD energies at megagauss fields there appear two serious difficulties.

(1) The 5L model does not describe perfectly the experimental free-electron energies in the megagauss field range (cf. Najda *et al.*, Refs. 25 and 26).

(2) There exists at present no MD theory within the framework of a 5L model. Such a calculation would be laborious and would require numerous approximations. There exists a description of MD energies for narrow-gap semiconductors,¹¹⁻¹³ but it is not directly applicable to the medium-gap materials since one may not assume that in the latter the $\mathbf{k}\cdot\mathbf{p}$ interaction across the fundamental $\Gamma_6-\Gamma_8$ gap is dominant.

In view of the above difficulties we treat the problem in the following way. First, we do not attempt to account for the absolute values of MD energies, but describe the MD energies *in relation* to the free-electron energies. Second, in order to use the existing MD theory based on the two-level (2L) $\mathbf{k}\cdot\mathbf{p}$ model, we describe the conduction bands of GaAs and InP by an effective 2L model. This is done by fitting the calculated and experimentally confirmed dispersion relation $E(k)$ for the conduction band into an effective 2L $\mathbf{k}\cdot\mathbf{p}$ formula,

$$\frac{\hbar^2 k^2}{2m_0^*} = E \left[1 + \frac{E}{\epsilon_g^*} \right], \quad (8)$$

in which the gap takes an adjusted value ϵ_g^* .²² The adjusted values of ϵ_g^* for GaAs and InP are 0.98 and 0.89 eV, respectively.^{22,23} This means that the conduction bands of the two materials are considerably more nonparabolic than one would infer from their real fundamental gaps $\epsilon_g = 1.51$ eV for GaAs and $\epsilon_g = 1.42$ eV for InP.

Taking into account the above simplifications the variational MD energies in effective Rydbergs are given in the form

$$E_{\pm} = -\frac{\epsilon_g^*}{2} + \left\{ \left[\frac{\epsilon_g^*}{2} \right]^2 + \epsilon_g^* \left[\langle K \rangle \pm \gamma \frac{m_0^*}{2m_0} (g_0^* - 2) \right] \right\}^{1/2} \pm \gamma \frac{m_0^*}{m_0} + \langle U \rangle, \quad (9)$$

where

$$K = -\nabla^2 - i\gamma \frac{\partial}{\partial \varphi} + \frac{\gamma^2 \rho^2}{4}. \quad (10)$$

Here m_0^* and g_0^* are the band-edge effective mass and the spin g value, respectively. The brackets $\langle K \rangle$ and $\langle U \rangle$ denote the variational averages of the kinetic energy (10) and the potential energy $U = -2/(\rho^2 + z^2)^{1/2}$. It is to be noticed that in the above formula the two energies do not appear on equal footing. Expression (9) follows from Eq. (11) of Ref. 13 in the limit of $E - U \ll \epsilon_g^* + \frac{2}{3}\Delta$, where Δ is the spin-orbit energy. In addition, the free-electron Pauli term with $g=2$ is explicitly retained (in Ry* units). This term is not negligible in the medium-gap materials, in contrast to the narrow-gap case. It can be easily checked that expanding the square root (in the limit of $K \ll \epsilon_g^*$) one obtains from (9) the standard expression for the orbital and spin quantization.

Thus, the calculation of MD energies amounts to separate evaluations of the trial averages $\langle K \rangle$ and $\langle U \rangle$ and a minimization of the energy (9). This is done with the use of (2) and (4) wave functions. The corresponding free-electron energies are calculated within the same model by putting in (9) the energies $\langle U \rangle = 0$ and $\langle K \rangle = 2\gamma(n + \frac{1}{2})$.

III. EXPERIMENTAL DATA

Magnetoabsorption experiments in megagauss magnetic fields have been described by Najda *et al.*^{24,25} The magnetic fields were generated by the single-turn-coil technique. The absolute field strength could be determined to an accuracy better than 2%. The field homogeneity was higher than $\pm 2\%$ at 1 mm off the coil center. The infrared radiation in the range from 9.2 to 10.8 μm was provided by an externally chopped cw CO₂ laser. The sample temperature could be reduced to approximately 15 K by flowing liquid helium around the cryostat. The data acquisition occurred several microseconds before the destruction of the coil. Several shots were performed under the same experimental conditions to ensure reproducibility of the results.

Infrared transmission experiments were performed on

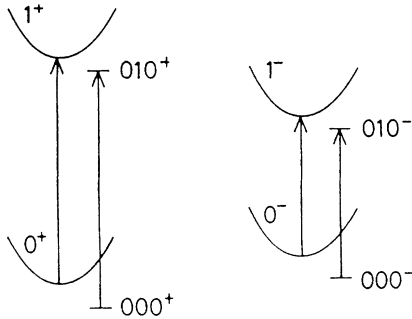


FIG. 2. Cyclotron resonance and impurity-shifted cyclotron resonance transitions for both spin orientations, as observed in GaAs at megagauss fields (schematically).

10- μm -thick GaAs sample prepared by vapor-phase epitaxy. The sample had the electron concentration $n = 1.5 \times 10^{16} \text{ cm}^{-3}$ and a mobility $\mu = 100\,000 \text{ cm}^2/\text{V sec}$ at 77 K. The experiments with InP were performed on two vapor-phase epitaxial samples. Sample 1 had an electron concentration $n = 1.5 \times 10^{16} \text{ cm}^{-3}$, a mobility of $23\,000 \text{ cm}^2/\text{V sec}$ at 77 K, and an epitaxial thickness $d = 17.3 \mu\text{m}$. For sample 2, the corresponding values were $n = 4.9 \times 10^{15} \text{ cm}^{-3}$, $\mu = 30\,000 \text{ cm}^2/\text{V sec}$ and $d = 14.2 \mu\text{m}$.

Figure 2 shows schematically the free-electron cyclotron resonance (CR) and the impurity cyclotron resonance (ICR) transitions in GaAs. As follows from the $5L \text{ k}\cdot\text{p}$ calculation for free electrons, the g value in GaAs at megagauss fields is negative for the $n=0$ Landau level and positive for the $n=1$ level.²⁴

Figure 3 shows magnetoabsorption traces measured on GaAs at a fixed-laser frequency. The decrease of

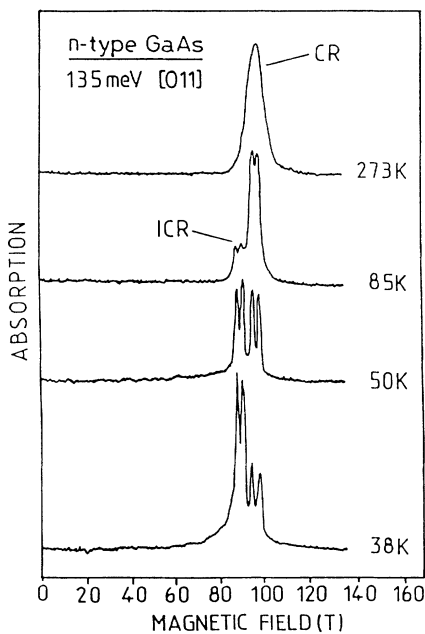


FIG. 3. Magnetoabsorption of GaAs vs field intensity for a constant laser wavelength. As the temperature is reduced magnetodonor transitions (ICR) become stronger.

transmission at the resonance amounts to a few percent. The evolution of the traces with increasing temperature allows one to discriminate between CR and ICR transitions. At low temperatures the donor transitions are stronger since the electrons occupy predominantly the ground MD state. The doublet structures correspond to spin-up and spin-down transitions, which do not have the same energies because the spin splitting of the $n=0$ Landau level is different from that of the $n=1$ level (cf. Fig. 2). For a given B value, the energy of the ICR transition between MD states (000) and (010) is higher than the energy of the corresponding CR transition, since the binding energy of the ground donor state (000) is larger than that of the excited (010) state (cf. Table I).

IV. RESULTS AND DISCUSSION

Figure 4 shows the energies of the CR and ICR transitions in GaAs, as measured in Ref. 24 for four CO_2 laser lines and two magnetic-field orientations. The solid and dashed straight lines are the least-square fits to the data. The fitting procedure is necessary since in order to compare the data with the theory one needs to know the transition energies for a given field, whereas experimentally one sweeps the field at a fixed-laser energy.

Figure 5 shows the magnetoabsorption traces for n -type InP at a fixed-laser frequency.²⁵ As in the case of GaAs, the temperature dependence of the traces allows one to differentiate between the CR and the ICR transitions. However, in contrast to the lower field data of Hopkins *et al.*²³ the spin doublets are not resolved. Figure 6 shows the energies of the CR and the ICR transitions for two InP samples versus magnetic field for five laser energies, as measured in Ref. 25. Again, the solid and dashed straight lines are the least-square fits to the data. Somewhat different results for the two samples give an idea of experimental uncertainties.

Since the theory does not account for the anisotropy for the MD energies with respect to field direction, we

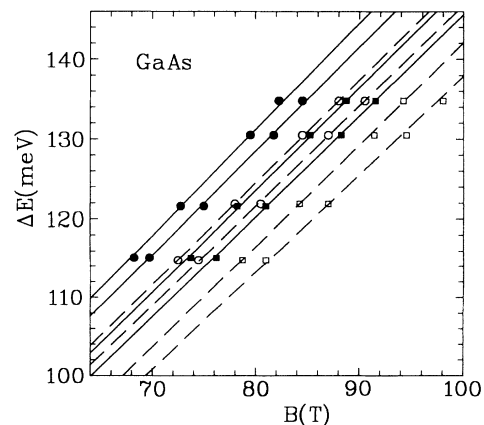


FIG. 4. CR and ICR transition energies in GaAs vs field intensity. Full signs (solid lines) are for $\mathbf{B} \parallel [011]$, open signs (dashed lines) are for $\mathbf{B} \perp [011]$. Free-electron transitions, squares; magnetodonor transitions, circles. The straight lines are the least-square fits to the data.

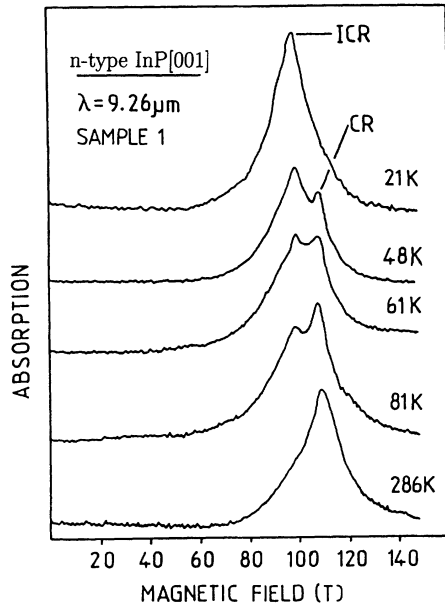


FIG. 5. Magnetoabsorption of InP for $\mathbf{B} \parallel [011]$ vs field intensity for a constant laser wavelength. As the temperature is reduced magnetodonor transitions (ICR) become stronger. The spin doublets are not resolved.

average the experimental data for CR and ICR energies in GaAs (as presented in Fig. 5) for $\bar{B} \parallel (001)$ and $\bar{B} \parallel (011)$ directions (separately for each spin) and obtain $\bar{E}_{\text{exp}}^{\pm}(\text{CR})$ and $\bar{E}_{\text{exp}}^{\pm}(\text{ICR})$. Figure 7 shows the energy differences $\bar{E}_{\text{exp}}^{\pm}(\text{ICR}) - \bar{E}_{\text{exp}}^{\pm}(\text{CR})$ by the dashed lines. The fact that the two lines do not coincide indicates that the spin g value for the MD states depends somewhat differently on n than that for the corresponding Landau levels. However, one should not attach much importance to this result since the nonaveraged experimental spin-doublet splittings do not exhibit any clear pattern either in relation to the field direction or between the ICR and the CR transitions. (It has been shown before, cf. Fig. 10 of Ref. 24, that the experiments in pulsed megagauss fields do not

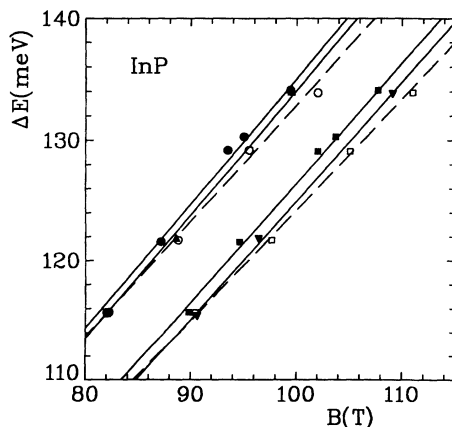


FIG. 6. CR and ICR transition energies in InP vs field intensity. Full signs (solid lines) are for $\mathbf{B} \parallel [011]$, open signs (dashed lines) are for $\mathbf{B} \parallel [011]$. Sample 1, squares; sample 2, triangles. The straight lines are the least-square fits to the data.

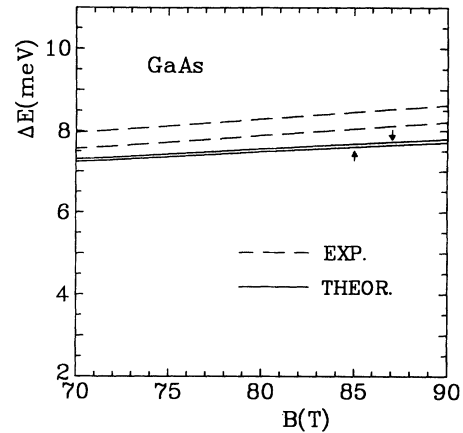


FIG. 7. Energy shifts between ICR and CR transitions in GaAs for both spin orientations vs field intensity. Dashed lines, experimental data; solid lines, theory.

discriminate between the free-electron spin-doublet splitting for different field orientations in GaAs).

Similar averaging procedure was used for InP to obtain the experimental values of $\bar{E}_{\text{exp}}^{\pm}(\text{ICR}) - \bar{E}_{\text{exp}}^{\pm}(\text{CR})$, as shown by the dashed line in Fig. 8. As in this case the spin doublets were not resolved, the lines for both spin directions coincide. The reason for the small splittings of the spin doublets in InP at high fields can be understood from the following considerations. Generally speaking, the energy dependence of the electron g value in III-V compounds runs from negative values at the band edge to the free-electron value $g=2$ at high energies (cf. Zawadzki, Ref. 26). This dependence is strongest in the narrow-gap material InSb ($g_0^* \approx -51$), somewhat weaker in InAs ($g_0^* \approx -15$), and it is still observable in GaAs ($g_0^* \approx -0.44$). In InP the band-edge g value is already positive ($g_0^* \approx +1.26$) and consequently its energy dependence is weak, since it quickly saturates at the value of $+2$. For this reason, the spin-doublet splitting, although observable at lower fields (cf. Ref. 23), becomes very small at high fields, (i.e., in the saturation regime).

In order to calculate the theoretical values of

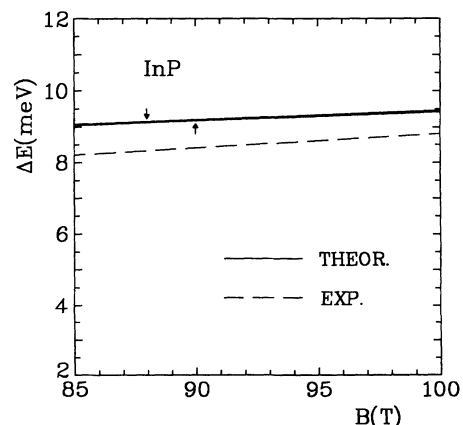


FIG. 8. Energy shifts between ICR and CR transitions in InP vs field intensity. Dashed lines, experimental data; solid lines, theory (the spin doublets almost coincide).

$E^{\pm}(\text{ICR}) - E(\text{CR})^{\pm}$ we use (9) with the variationally calculated energies of (000) and (010) MD states, and put $U=0$ and $K=2\gamma(n+\frac{1}{2})$ for the free-electron states. In the computations we used the following values of the material parameters. For GaAs:²² $m_0^* = 0.0660m_0$, $g_0^* = -0.44$, $\epsilon_g^* = 0.98$ eV, and $\text{Ry}^* = 5.8$ meV. For InP:²³ $m_0^* = 0.0793m_0$, $g_0^* = +1.26$, $\epsilon_g^* = 0.89$ eV, and $\text{Ry}^* = 7.7$ meV. The resulting theoretical values of $E_{\text{th}}^{\pm}(\text{ICR}) - E_{\text{th}}^{\pm}(\text{CR})$ are shown in Fig. 7 for GaAs and in Fig. 8 for InP by the solid lines.

Taking into account the uncertainties of the experiment as well as the approximations of the theory, the overall agreement between the two should be considered good: both the absolute values and the slopes of field dependences are reproduced quite well. Small discrepancies of the absolute values could be corrected by slight changes of the Ry^* values, which are not known to an accuracy better than 10%. It can be seen that in the case of GaAs the experimental values of the spin-doublet splittings are larger than the theoretical estimates. However, neither the experiment nor the theory is sufficiently precise in this respect. It has been mentioned above that the spin-doublet splittings of ICR and CR peaks in pulsed megagauss fields do not exhibit any regular pattern. This is in contrast to the lower dc field experiments on GaAs, where the ICR splittings are slightly but distinctly smaller than the CR ones (cf. Fig. 3 of Ref. 9). As to the theory, formula (9), based on the effective $2L$ $\mathbf{k}\cdot\mathbf{p}$ model (8), describes well the orbital electron properties but less well the spin properties. Retaining the Pauli free-electron term outside the square root in (9), we reproduce the change of sign of the g value between $n=0$ and 1 Landau levels, which really occurs in GaAs according to

the $5L$ model. In fact, using (9) and the above GaAs parameters one obtains for $B=80$ T: $g^*(0) = -0.15$ and $g^*(1) = +0.21$. The corresponding values, calculated according to the $5L$ model²⁴ and averaged over [001] and [011] field directions, are $g^*(0) = -0.051$ and $g^*(1) = +0.48$. Thus, the effective $2L$ formula (9) gives reasonable but not precise g values for the levels of our interest. The spin doublets of the CR transitions in GaAs have been successfully described by the $5L$ $\mathbf{k}\cdot\mathbf{p}$ model both at moderate and megagauss fields.^{22,24} In order to achieve the same precision in the description of spin doublets for magnetodonor transitions, one would have to solve the $5L$ model for the impurity states, a task we have not attempted. Thus, the problem of spin splittings of MD states in GaAs requires further experimental and theoretical effort.

As argued above, the spin-doublet splittings in InP should be much smaller than in GaAs. The calculation confirms this prediction; it can be seen in Fig. 8 that the theoretical lines for the two spin orientations almost coincide. It is not quite clear whether the absence of experimental spin doublets in InP at megagauss fields, as shown in Fig. 5, should be entirely attributed to the fact that at high fields the g factors for both Landau and MD levels saturate at the free-electron value of $+2$, or partly at least to a lower resolution of the pulsed-field results, as compared to the dc data.²³

ACKNOWLEDGMENT

One of us (W.Z.) thanks Professor Günther Bauer for generous hospitality during his stay in Linz.

*Permanent address: Institute of Physics, Polish Academy of Sciences, 02-668 Warsaw, Poland.

†Present address: Sharp Laboratories of Europe, Oxford OX4 4GA, United Kingdom.

¹G. E. Stillman, C. M. Wolfe, and J. O. Dimmock, in *Semiconductors and Semimetals*, edited by R. K. Willardson and A. C. Beer (Academic, New York, 1977), Vol. 12, p. 169.

²Y. Yafet, R. W. Keyes, and E. N. Adams, *J. Phys. Chem. Solids* **1**, 137 (1956).

³C. L. Littler, W. Zawadzki, M. R. Loloee, X. N. Song, and D. G. Seiler, *Phys. Rev. Lett.* **63**, 2845 (1989).

⁴W. Zawadzki, in *Landau Level Spectroscopy*, edited by G. Landwehr and E. I. Rashba (Elsevier, Amsterdam, 1991), p. 1305.

⁵R. Kaplan, in *Optical Properties of Solids*, edited by E. D. Haidemenakis (Gordon and Breach, New York, 1970), p. 322.

⁶T. O. Poehler, *Phys. Rev. B* **4**, 1223 (1971).

⁷A. Kadri, K. Zitouni, L. Konczewicz, and R. L. Aulombard, *Phys. Rev. B* **35**, 6260 (1987).

⁸H. Sigg, H. Y. A. Bluysen, and P. Wyder, *Solid State Commun.* **48**, 897 (1983).

⁹W. Zawadzki, P. Pfeffer, and H. Sigg, *Solid State Commun.* **53**, 777 (1985).

¹⁰C. Y. Armistead, R. A. Stradling, and Z. Wasilewski, *Semicond. Sci. Technol.* **4**, 557 (1989).

¹¹D. J. Larsen, *J. Phys. Chem. Solids* **29**, 271 (1968).

¹²W. Zawadzki and J. Wlasak, in *Theoretical Aspects and New Developments in Magneto-Optics*, edited by J. T. Devreese (Plenum, New York, 1980), p. 347.

¹³W. Zawadzki, X. N. Song, C. L. Littler, and D. G. Seiler, *Phys. Rev. B* **42**, 5260 (1990).

¹⁴J. M. Mercy, Y. H. Chang, A. A. Reeder, G. Brozak, and B. D. McCombe, *Superlatt. Microstruct.* **4**, 213 (1988).

¹⁵J. P. Cheng and B. D. McCombe, *Phys. Rev. B* **42**, 7626 (1990).

¹⁶R. L. Green and K. K. Bajaj, *Phys. Rev. B* **31**, 913 (1985).

¹⁷J. L. Robert *et al.*, *Phys. Rev. B* **33**, 5935 (1986).

¹⁸W. Zawadzki, M. Kubisa, A. Raymond, J. L. Robert, and J. R. Andre, *Phys. Rev. B* **36**, 9297 (1987).

¹⁹E. M. Pokatilov and M. M. Rusanov, *Fiz. Tverd. Tela (Leningrad)* **10**, 3117 (1968) [*Sov. Phys. Solid State* **10**, 2458 (1968)].

²⁰J. A. C. Gallas, *J. Phys. B* **18**, 2119 (1985).

²¹W. E. Rösner, H. Wunner, H. Herold, and H. Ruder, *J. Phys. B* **17**, 29 (1984).

²²P. Pfeffer and W. Zawadzki, *Phys. Rev. B* **41**, 1561 (1990).

²³M. A. Hopkins *et al.*, *Semicond. Sci. Technol.* **2**, 568 (1987).

²⁴S. P. Najda, S. Takeyama, N. Miura, P. Pfeffer, and W. Zawadzki, *Phys. Rev. B* **40**, 6189 (1989).

²⁵S. P. Najda, H. Yokoi, S. Takeyama, N. Miura, and P. Pfeffer, *Phys. Rev. B* **44**, 1087 (1991).

²⁶W. Zawadzki, *Phys. Lett.* **4**, 190 (1963).